ELECTRICALLY INDUCED STRIP WAVEGUIDE MODES

I. SAVATINOVA, S. TONCHEV, E. POPOV and L. MASHEV
Institute of Solid State Physics, Bulgarian Academy of Sciences, boul. Lenin 72, 1784 Sofia, Bulgaria

Received 2 October 1987; revised manuscript received 26 January 1988

Numerical results of the dispersion characteristics and field distribution of the transverse modes of an electrically induced strip waveguide with gaussian refractive index depth profile are presented. Cut-off conditions are discussed in connection with the transverse energy localization.

1. Introduction

Recently Yamamoto et al. [1] have demonstrated experimentally that light can be confined into a thin film only by a partial cladding with metal strips. Far-field pattern of several transverse modes have been demonstrated using Al_2O_3 layer on a SiO_2/Si-substrate. In the same time, an electrically induced optical waveguide has been formed using a pair of electrodes deposited on electrooptic single crystals. The applied voltage (≈ 4 V/μm in the case of $LiNbO_3$ [2] and 3 V/μm in the case of $KNbO_3$ [3]) provides cut-off modulation.

Replacing the pure $LiNbO_3$ substrate with a Ti:$LiNbO_3$ waveguide, such electrooptic effect can be observed at much lower voltages [4], due to the light localization in the guide depth. It is worth noting that in this case both the amplitude and the phase of the guided light propagating in the electrode gap can be changed. An effective amplitude modulation and beam-splitting have been demonstrated in ref. [4].

The purpose of this paper is to investigate the characteristics of electrically induced strip waveguide transverse modes. The influence of the metal electrodes and the applied voltage on the effective refractive indices and the field distribution of the modes are discussed in detail.

2. Presentation of the physical problem

The structure under consideration is presented schematically in fig. 1. The waveguide and electrode parameters at wavelength $\lambda = 0.6328$ μm are given in table 1. We have considered a planar Y-cut Ti:LiNbO waveguide with a gaussian refractive index profile

$$n(y) = n_0 + \Delta n \exp(-y^2/D^2) , \qquad (1)$$

where D is the waveguide effective thickness, n_0 and

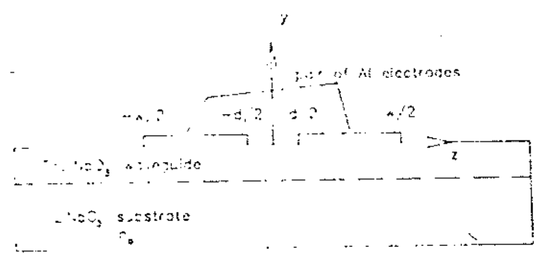

Fig. 1. An electrically induced channel in Ti:$LiNbO_3$ planar waveguide.

Table 1
Structure parameters

waveguide	electrodes
$n_b = 2.2003$	$w = 50$ μm
$\Delta n = 0.0016$	$d = 10$ μm
$D = 0.9$ μm	$L = 5$ mm
$n^0_{eff} = 2.20195$	
$n^M_{eff} = 2.20160$	

0 030-4018/88/$03.50 © Elsevier Science Publishers B.V.
(North-Holland Physics Publishing Division)

n_b are the refractive indices at the surface and of the substrate respectively and $\Delta n = n_0 - n_b$. The set of waveguide parameters provides the existence of only the TE_0 depth mode with an effective refractive index n^0_{eff}. An applied voltage U between the two electrodes increases the waveguide refractive index according to

$$\Delta n^E(y, z) = r_{33} n^3 E_z / 2 , \qquad (2)$$

where the electric field distribution is given by [5]

$$E_z = \frac{U}{2wK(w/d)\,\mathrm{Re}\{[[1-(v/d)^2][1-(v/w)^2]]^{1/2}\}}, \qquad (3)$$

where K is the elliptical integral of the first kind, and $v = z + iy$.

In the electrically induced strip waveguide, light tends to propagate in the gap between the electrodes because of the "$+\Delta n$"-channel formed by the additive influence of the metal cladding Δn^M_{eff} and the electrooptic effect Δn^E_{eff}. Therefore the external electric field can be used to enhance the optical strip line effect. The shape of the lateral refractive index profile is similar to that of the so-called W-fibers, where a high index core is surrounded by two layers with different indices. Tow symmetric potential barriers round the central gap are formed under the metal-clad regions. Such a system is a self-filtering waveguide [6] which looses the higher-order modes. In our configuration all modes are more or less leaky: the fundamental one being the best confined. Thus the channel contains a small amount of modes with effective mode indices $n^{ch}_{eff} > n^M_{eff}$, where $n^M_{eff} = n^0_{eff} - \Delta n^M_{eff}$ is the depth mode effective index value under the metal layer.

3. Numerical procedure

Since in the presence of electrodes the refractive index distribution is a function of two variables, y and z, the problem becomes two-dimensional (2-D). A set of 2-D partial differential equations can be solved rigorously by a 2-D numerical integration using the finite-difference method. In the case of small lateral refractive index fluctuations, however, the method of effective refractive indices [7] can be applied efficiently for a step-index distribution. In order to suit it to the case of gradient index profile, we have combined the effective index method with the matrix method, used for analysis of multilayered planar waveguides [8]. The calculation scheme is the following.

(i) The gaussian refractive index profile of the planar waveguide is represented as a step-like N-layer structure. Its mode propagation constant is calculated by a matrix method [8]. Table 2 shows the convergence of the mode effective index to n^0_{eff} of the initial gradient waveguide as a function of N. Furtheron in the calculations we have taken $N = 100$.

(ii) According to eqs. (2) and (3), the applied voltage changes the refractive indices of each of the N layers in the z-direction. A depth mode index has been calculated for each value of z in the same way as for $U = 0$ V, using the corresponding modified values of $n(y, z)$. The interval $z \in [-50, 50]$ has been divided into 1000 parts.

(iii) Representing the depth mode index distribution in z as a stack of 1000 layers, the matrix method is applied for the calculation of the transverse mode indices and fields.

(iv) The procedures (ii) and (iii) are repeated, inserting another value of U.

Two peculiarities have to be pointed out.

(i) Due to the complex refractive index of the aluminum, the mode effective indices are complex too. Thus the calculations of the zero of the characteristic matrix have to be performed in the complex n_{eff}-plane. The most powerful method for the search for zeroes proves to be Newton iterative procedure, generalized for complex variables.

Table 2
Convergence rate

N	$\mathrm{Re}(n^0_{eff})$
4	2.20278
10	2.20264
20	2.20250
50	2.20235
70	2.20208
80	2.20196
90	2.20195
100	2.20195

(ii) In the investigated region of $U \in 0$–60 V the depth mode propagation constant is practically a linear function of U and can be represented in the form

$$n_{\rm eff}(z, U) \approx n_{\rm eff}/_{u=0} + U\,\partial n_{\rm eff}/\partial U\,. \qquad (4)$$

This fact facilitates to a great extend the calculation, since only the values of $\partial n_{\rm eff}/\partial U$ as a function of z are sufficient, calculated only at a certain value of U.

4. Results

Fig. 2 shows the influence both of the metal coating and the electrooptic effect on the depth mode effective index. The great negative real part of the Al dielectric constant diminishes the depth mode effective index and leads to the partial localization of the optical field. On the anoither hand 10 V across 10 μm electrode distance provides an index variation $\Delta n_{\rm eff}^{E} \approx 10^{-4}$ which is comparable to $\Delta n_{\rm eff}^{M}$, associated with the metal overlay. An important feature of the structure in fig. 2 is that mainly even modes with maximal field amplitude along the guide axis can be excited. Applying higher voltages, $n_{\rm eff}^{02}$ increases and some of the leaky modes can pass to the normal ones. The behavior of $n_{\rm eff}^{00}$ and $n_{\rm eff}^{02}$ calculated as a function of U is displayed in fig. 3. At low voltages the second

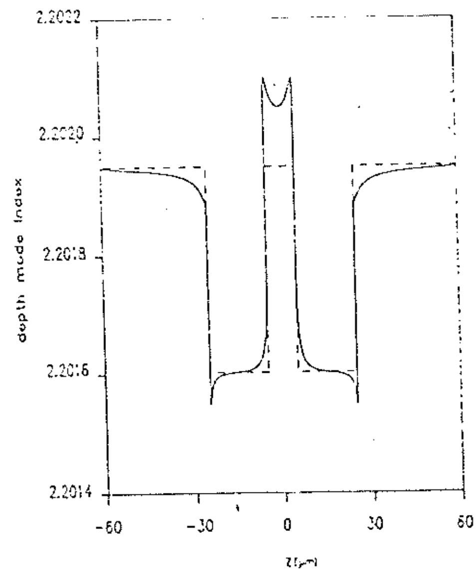

Fig. 2. Real part of the depth mode effective index distribution. Dashed curve, $U=0$ V; solid curve, $U=10$ V.

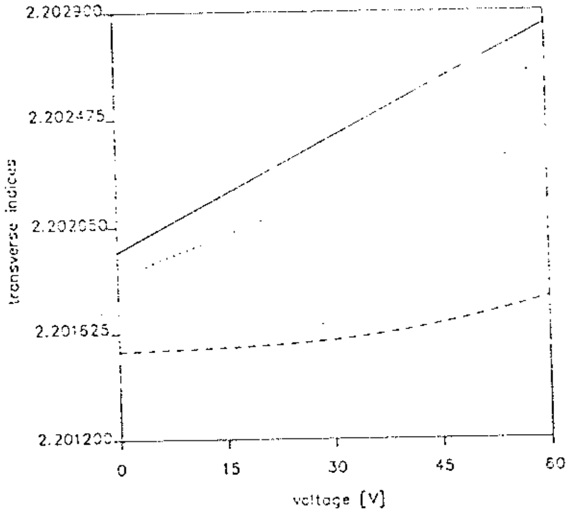

Fig. 3. Variation of the transverse mode indices $n_{\rm eff}^{00}$ (with dotted curve) and $n_{\rm eff}^{02}$ (with dashed curve) as a function of the applied voltage. The maximum refractive index change is shown with solid curve.

even mode is leaky, but at $U \geqslant 30$ V its effective index exceeds the critical level $n_{\rm eff}^{M}$.

More impressive is the picture of the mode fields, given in fig. 4. The fundamental mode remains well confined in the voltage interval 0–60 V, but the evolution of the second even mode is drastic. Its field amplitude flows to the electrode gap center rather quickly, making the coincidence with the fundamen-

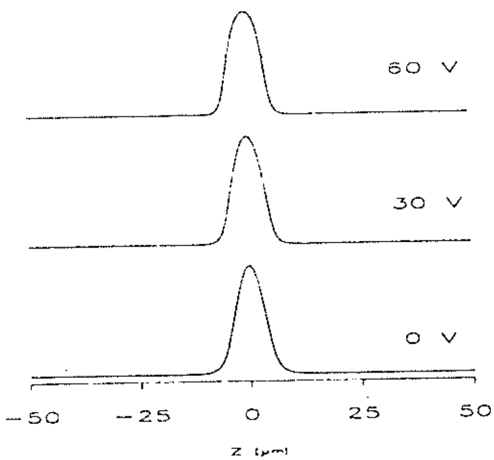

Fig. 4. Optical mode intensity distribution of an electrically induced strip waveguide. Solid curve, TE_{00} mode; dotted curve, TE_{02} mode.

tal amplitude more complete. It must be pointed out that cut-off conditions $n_{eff}^{02} > n_{eff}^{M}$ is not a rigorous one: in fact truly bound between the electrodes are modes characterized with $n_{eff}^{02} > n_{eff}^{0}$, the only modes that are not radiated towards $z \to \mp\infty$. Nevertheless, if $n_{eff}^{02} > n_{eff}^{M}$, the mode field is located near the electrode gap and as its effective index grows up the energy flow towards $z \to \mp\infty$ becomes more and more neglectible. Moreover, since the depth of the symmetrical potential barriers under the electrodes increases with U, even modes with $n_{eff}^{02} \approx n_{eff}^{M}$ are confined. In fact the most important criterion is the ratio between the "bounded" and "radiated" energy. In fig. 5 the transverse distribution of the intensity of TE_{02} mode is shown in the region $0 \le U \le 20$ V. The following conclusions can be drawn:

(i) for $U=0$ V the value of the intensity maximum is comparable with the intensity of the radiated field (the ratio not exceeding a value of 4);

(ii) above $U \ge 10$ V that ratio exceeds 10 and the radiated energy can be neglected, in comparison to the bound one between and below the electrodes, though for $U \le 30$ V $n_{eff}^{02} < n_{eff}^{M}$. Moreover, a peak in the center region is formed and it can interfere with the field of TE_{00} mode, depending on their phase difference.

It is well known that the modes of an infinite-length waveguide can not interfere with each other because of their orthogonallity. The presence of a physical boundary (or the waveguide edge), however, cancels this requirement. The interference between the even modes results in oscillations of the output intensity with a high extinction ratio. Thus an amplitude modulation can occur at the end of the electrode region in x. If the length of the electrodes is L, and if we assume a constant and optimum excitation conditions for both TE_{00} and TE_{02} modes, the output intensity would depend on the difference between their phases after a path of L along the electrodes,

$$\Delta\varphi(U, L) = (2\pi/\lambda)\ [n_{eff}^{00}(U) - n_{eff}^{02}(U)]L\ . \qquad (5)$$

Assuming an independence of the initial phase difference $\Delta\varphi(U, 0)$ on U, the voltage change ΔU necessary to obtain a transition from a minimum to a maximum is defined by

$$\Delta\varphi(U+\Delta U, L) - \Delta\varphi(U, L) = \pi\ . \qquad (6)$$

The results presented in fig. 3 allow us to assume that n_{eff}^{02} is practically independent on U in comparison with the change of n_{eff}^{00}. In that case condition (6) can be represented as

$$n_{eff}^{00}(U+\Delta U) - n_{eff}^{00}(U) = \lambda/2L\ . \qquad (7)$$

Numerical results (fig. 3) enables us to interpolate n_{eff}^{00} as a linear function of U,

$$n_{eff}^{00}(U) = n_{eff}^{00}(0) + qU\ , \qquad (8)$$

with

$$q \approx 1.1 \times 10^{-5} [V^{-1}]\ . \qquad (9)$$

Substituting of (8) and (9) in eq. (7) with $\lambda = 0.6328$ μm and $L = 5$ mm results in

$$\Delta U = \lambda/2qL \approx 5.75\ \text{V}\ . \qquad (10)$$

To illustrate that phenomenon a waveguide with the same parameters as in table 1 was prepared. When a DC voltage is applied to the electrodes, a sequence of maxima and minima of the output intensity has been observed (fig. 6). A saw-tooth generator was used as a voltage source. The output intensity was measured with a detector located in the center of the pq-lines picture. A maximum modulation efficiency up to 95% was achieved under optimum excitation conditions. The half-wave voltage was estimated to be about 7 V, in a good agreement with the theoretical value (10).

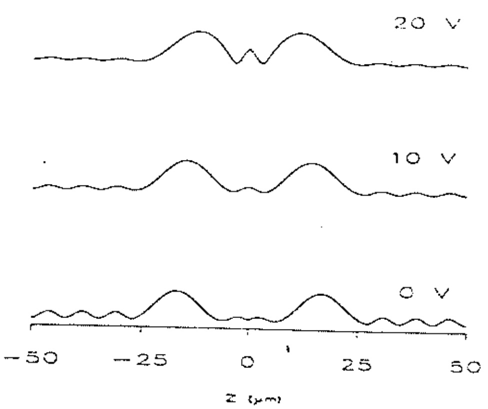

Fig. 5. Transverse distribution of TE_{02} mode intensity for $U=0$ V, $U=10$ V and $U=20$ V.

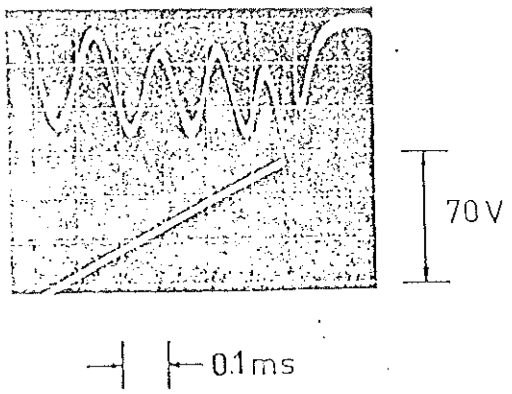

Fig. 6. Modulator response: upper trace – detected light signal, lower trace – modulating signal.

. Discussion

If a weak non-linearity of $n_{eff}^{00}(U)$ and a slow variation of $n_{eff}^{02}(U)$ are taken into account, a small change of the half-wave voltage ΔU with increase of U can be expected. Higher modes excitation would have a weak influence on the process, too.

Despite the obtained agreement between the theoretical and experimental values ΔU we refrain from the conclusion that there is a quantative, rather than qualitative experimental confirmation of the theoretical considerations, because of the existence of one question that needs further investigations: In order to achieve a great value of the modulation depth in the entire voltage range (fig. 6), the central peaks of TE_{00} and TE_{02} mode fields have to be almost identical, contrary to fig. 4 and fig. 5. There are two possible explanations.

(i) From an experimental point of view: if the excitation conditions are more optimal for TE_{02} mode, it would compensate the greater value of TE_{00} field at $z=0$.

(ii) From a theoretical point of view: the waveguide parameters ($\Delta n = 0.0016$ and $D = 0.9$ μm) in the calculations may not correspond exactly to the experimental ones, although n_{eff}^{0} is the same. Furthermore, if the imaginary part of the refractive index n_{Al} of the metal electrodes has a higher value (n_{Al} depends on the deposition process), the electrodes can have a stronger influence on n_{eff}^{0}, thus TE_{02} can be more confined between them even without applied voltage.

Acknowledgements

This research has been completed with the financial support of the Committee for Science at the Council of Ministers under contract No 114.

References

[1] Y. Yamamoto, T. Kamiya and H. Yanai, Appl. Optics 14 (1975) 322.
[2] D.J. Channing, Appl. Phys. Lett. 19 (1971) 128.
[3] J.C. Baumert, C. Walter, P. Buchmann, H. Melchior and P. Gunter, Proc. Third Europian Conf. on Integrated optics, ECIO'85, Berlin, (1985) p. 44.
[4] I. Savatinova, S. Tonchev, Kh. Pushkarov and F. Scharf, J. Opt. Commun. 5 (1985) 10.
[5] O.G. Ramer, IEEE J. Quant. Electr. QE-18 (1982) 393.
[6] V.V. Cherny, G.A. Juravlev, A.I. Kipra and V.P. Tjoy, SPIE Guided Wave Optical Systems and Devices II, V 176 (1979) p. 173.
[7] G. Hocker, W.K. Burns, Appl. Optics 16 (1977) 113.
[8] E. Popov and L. Mashev, Optics Comm. 52 (1985) 393.